Surface flow visualisation over forward facing steps with varying yaw angle

J Rowcroft[1], D Burton, HM Blackburn and J Sheridan

School of Mechanical and Aerospace Engineering, Monash University, Clayton, Australia

E-mail: jerome.rowcroft@monash.edu

Abstract. Many Australian wind farms are located near escarpments and cliffs where flow separation occurs. An absence of literature addressing the effect of wind direction over cliffs have motivated surface shear stress visualisations on forward facing steps at yaw angles between 0° and 50°. These visualisations have been conducted in the Monash University 450 kW wind tunnel. Mean reattachment lengths were measured and shown to vary as a function of the boundary layer thickness to step height ratio and the yaw angle. Vortices shed off the crest of the step induced surface shear stresses on the top surface of the step. The orientation of these shear stresses varied linearly with the yaw angle. Three-dimensional structures of different forms were also observed. At zero yaw angle the flow converged at points along the crest. At high yaw angles distinct sections of misaligned flow were observed downstream of the reattachment line, indicating a spatial periodicity in shedding.

1. Introduction

Siting wind turbines in the vicinity of escarpments, cliffs and ridges steep enough to cause flow separation is common in Australian wind farms, particularly in coastal cliff areas, as developers seek to take advantage of the speed-up generated by up-slopes associated with coastal cliffs. The research described here was initiated and partially funded by several wind energy companies to (a) identify problems with such an approach (b) optimize the siting of turbines placed in wind farms in such landscapes and (c) to develop design methods for such installations.

Many of these cliffs can be approximated by a Forward Facing Step (FFS). Depending on their upstream angle, FFSs can have downstream separation regions, where flow separates off the crest. The resulting vortices can buffet turbines placed in close proximity to the steps. A diagram of an FFS is presented in Figure 1.

Various researchers, including recent work by Ren and Wu [1], Sherry et al. [2], and Largeau and Moriniere [3], have quantified the size of the downstream separation region and parameterised the speed up and turbulence intensity (TI). A key parameter affecting the size and behaviour of the separation bubble is the ratio of boundary layer thickness to step height (δ/h). Largeau and Moriniere [3], comparing the work of Moss and Baker [4], Mohsen [5], Tashie et al. [6] and Farabee and Casarella [7], state that the size of the separation bubble increases as δ/h is reduced, and that the effect is more significant where δ/h is greater than 1. They suggest that this is due to the interaction between

---

[1] To whom any correspondence should be addressed.

the separation bubble and the up-stream flow TI, which will be higher closer to the surface. The other factor considered is whether the separation bubble is fully contained by the boundary layer.

There is limited data on the flow over a FFS as a function of direction. Baker [8] proposes that only flow perpendicular to an escarpment is accelerated and his own experimental work showed that this is a reasonable assumption. However, the analysis of yawed flow has not been researched to the extent that the FFS at 0° yaw angle (θ) has.

Sherry et al. [2] performed water channel experiments on flow over a FFS for a range of Reynolds numbers from 1400 to 19000. They observed that, in this Reynolds number range, the size of the downstream recirculation region became largely insensitive to Reynolds number above a critical Reynolds number of 8500. However, the size of the separation region does vary as a function of δ/h. Also, the size of the separation region becomes less dependent on the flow speed when the component of the flow perpendicular to the escarpment results in a Reynolds number greater than the critical Reynolds number. Thus, if Baker's [8] assumption is correct, the size of the downstream recirculation region would extend a constant distance downstream from the crest of the escarpment independent of the flow speed and hence θ, since θ changes the component of the flow perpendicular to the escarpment.

Largeau and Moriniere [3] studied flow over an FFS in an open jet wind tunnel, operating over the Reynolds number range of 2880 to 1.3×10^5. They observed that the accumulation of fluid in the upstream recirculation region occurred at a faster rate than could be drained laterally, thus forcing the flow over the crest of the step. Kiya and Sasaki [9], observing flow over a flat plate at Reynolds number of 26 000 in low turbulence conditions, described a similar forcing in terms of the growth of the downstream recirculation region, where it reaches a maximum containable size before fluid is ejected, giving the recirculation region a flapping appearance. This explanation of the separation and shedding mechanisms implies a relationship between the size of the mean recirculation region and the TI. An increase in TI would render the separation region unstable, giving it a propensity to shed sooner, resulting in a smaller mean reattachment length (X_L).
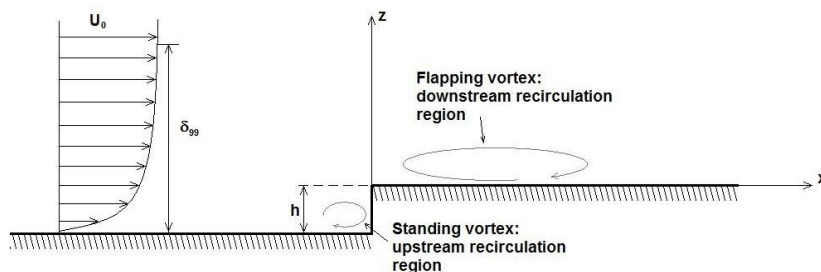

Figure 1. Diagram of forward facing step.

This research focuses first on the θ = 0° case, comparing X_L with previously published literature. Adjustment of θ in the low TI cases is then considered, covering a range of δ/h from 0.9 to 2.7. This analysis will identify the changes to X_L as a function of θ and δ/h, providing insight into the physical understanding of the flow processes. A similar analysis is then conducted with in-flow conditions comparable to a real-world atmospheric boundary layer, with δ/h in the range 4.77 to 14.3. A comparison is also made between the low and high TI cases.

2. Experimental setup
The research was conducted in the Monash University 450 kW wind tunnel, a schematic of which is shown in Figure 2. The wind tunnel is fan blade pitch controlled. The working section of the tunnel has a 2 m x 2 m cross-section and extends 12 m, as shown in Figure 2. Testing was completed in the centre region of the working section over FFS models of height $h = 0.050$ m, 0.100 m and 0.150 m at a nominal free-stream speed of 33 ms^{-1}.

The experiments were completed at Reynolds Numbers of 1 x 10^5, 2 x 10^5 and 3 x 10^5, using the step height, h, as the reference length. End plates extending upstream $12h$ upstream of the crest were used when $h = 0.050$ m. An example of the $h = 0.050$ m, $\theta = 20°$ yaw case is shown in Figure 3.

The FFS models of height 0.050 m, 0.100 m and 0.150 m resulted in 2.5%, 5% and 10% blockage. The yaw angles investigated were 0° to 50° in 10° increments. The models extended beyond $10h$ downstream, and can be thus considered isolated cliffs according to Moss and Baker [4].

The aspect ratio at $\theta = 0°$, defined as the ratio of model width to model height, following the work of de Brederode et al. [10] was maintained above 10. In the $h = 0.150$ m case, the aspect ratio was 13.3, while in the $h = 0.050$ m case with end plates, the aspect ratio was 34.

2.1. Inflow Conditions
Three sets of in-flow conditions were used; two with low TI, and a third with higher TI, and a thicker boundary layer. The vertical velocity and turbulence intensity profiles are shown in Figure 4. The inflow conditions were measured using a *TFI* four-hole pressure probe, with a 45° cone of acceptance. A sample time of 20 s and a sampling frequency of 2500 Hz were used.
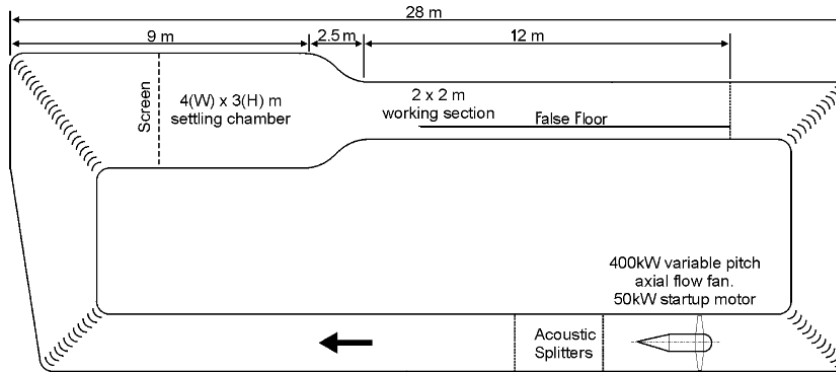

Figure 2. Schematic of the Monash University 450 kW wind tunnel.

Figure 3. (Left) Surface shear stress visualisation setup. Flow is from bottom to top. Step height is 50 mm. End plates are used. (Right) Trapezoidal vortex generator used to increase boundary layer thickness and turbulence intensity.

The low TI configurations were generated without any flow conditioners. In the first case, the step was located on the wind tunnel floor, a minimum of $42h$ downstream of the contraction, resulting in a δ of 0.135 m with free-stream TI of 1%. The second low TI configuration was developed over a false floor, with a fetch of $32h$. The resulting free-stream TI was also 1% and the δ was 0.100 m.

The high TI case was generated using a trapezoidal vortex generator at the entrance to the working section, as depicted in the right pane of Figure 3. This generated a δ of 0.715 m and free-stream TI below 5%. Figure 5 provides a comparison with a terrain category 1.5 (TC 1.5) boundary layer from the Australian Wind Loading Standard [11], representative of a coastal inflow conditions at a scale of 1:500. The velocity match is excellent, while the TI is lower than the standard. The modelled FFSs correspond to 25 m, 50 m, and 75 m in full scale.

Results from these configurations indicated significant wall effects and concerns regarding the aspect ratio (width to step height) with the 0.100 m and 0.150 m step heights. End plates were implemented in the $h = 0.050$ m case to negate the wall effects. The lower h increased the aspect ratio.

Lateral profiles were measured at a height of $\delta/2$; across a 0.500 m span, turbulence intensity and velocity measurements remained within a ±10% envelope. The second low TI configuration, conducted on the false floor, yielded a lateral inflow variation envelope of less than ±3.5%.
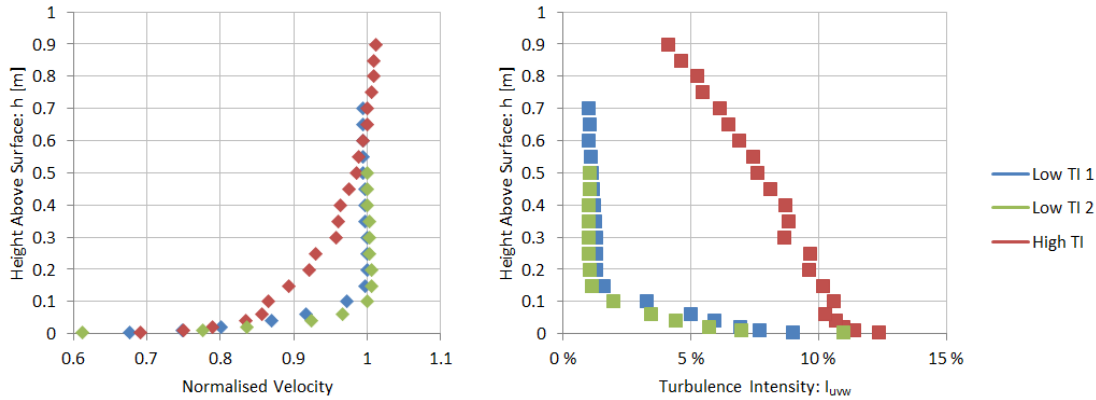

Figure 4. Vertical profiles of normalised velocity (Left) and turbulence intensity (Right) centreline profiles of the three inflows used.
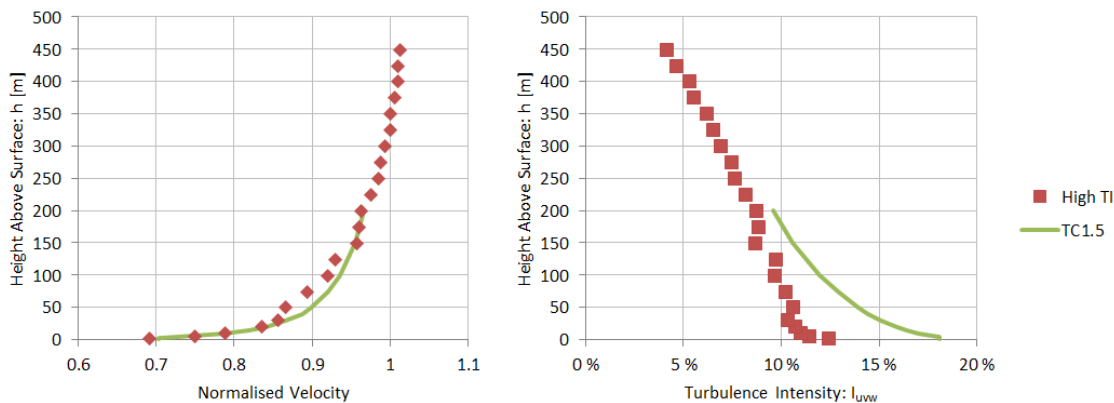

Figure 5. Vertical centreline profiles of normalised velocity (Left) and turbulence intensity (Right) of the high TI inflow configuration, compared against the TC 1.5 boundary layer. [11]

2.2. Description of flow visualisation technique
Arrays of paint droplets were used to visualise the surface shear stress over the downstream region of the FFS. The orientation of the paint streaks indicate the direction of the surface shear stress, allowing flow topology lines such as mean reattachment lines to be identified and the length of vortex regions to be measured. The mean reattachment line is defined as the line where the mean surface shear stress changes from acting in the direction of the crest (recirculation) to a direction away from the crest. The mean reattachment length is the distance from the crest of the FFS to the reattachment line.

The models were placed in the middle of the working section of the wind tunnel. The surfaces of the models were aerodynamically smooth, covered with a black semi-gloss surface, and gridded using a permanent marker. For the 0.100 m and 0.150 m FFSs, the grid had a lateral resolution of 0.100 m and a downstream resolution of 0.050 m. In the 0.050 m case lateral resolution of 0.025 m and stream-wise resolution of 0.010 m were used. This resulted in an uncertainty in X_L of $10 - 15\%$.

Magenta-coloured water-based paint was diluted with water to approximately a 1:1 ratio providing a mixture with sufficient viscosity to avoid speckling, but not so viscous as to stop the droplets from streaking. Hypodermic syringes were utilised to apply nominally 0.1 mL of the paint solution at each grid point in the 0.100 m and 0.150 m FFS cases. Further drops were applied at grid midpoints through the central region and towards the edges. This was done to increase the resolution so as to more precisely determine reattachment lengths, and to observe in more detail the edge effects. For $h = 0.050$ m, paint was administered to one in every four grid points in a diagonal array. The application of paint was performed in still conditions.

To obtain the streaks, the wind tunnel was run up to a fan blade pitch angle of 30°, corresponding to a free-stream velocity of 33 ms^{-1}. The wind tunnel was allowed to run at speed for approximately one minute from the time the wind tunnel fan blade pitch had reached 30°. This allowed the droplets sufficient time to form streaks.

3. Comparison with previous FFS work

Reattachment lengths were measured using the paint drop surface shear stress visualisation technique described in Section 2.2. An example is depicted in Figure 6. The direction of the streaks is clearly visible; the mean reattachment line is shown with a red dashed line.
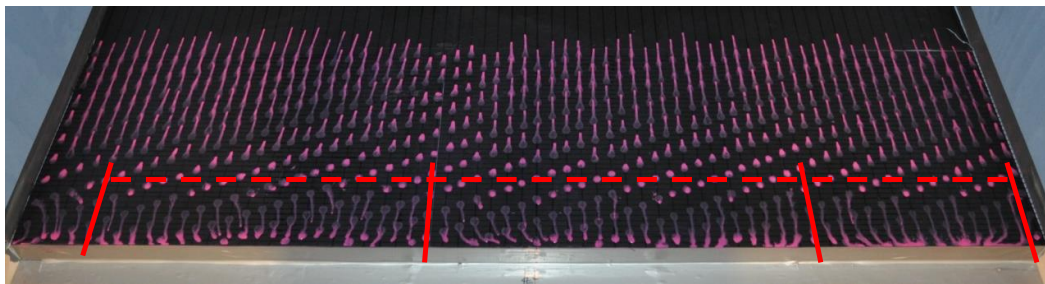

Figure 6. Surface shear stress visualisation of flow over a 50 mm FFS with δ/h = 2.7. Flow is from bottom to top. Notice the change in streak direction and the stagnation region 2.6h downstream of the crest, signifying the mean reattachment length. Note also the lateral component of the flow at the crest, indicating a cellular structure.

Reattachment lengths from the θ = 0° case are presented in Figure 7 and compared with values from other studies. Data from the current study are in good agreement with Farabee and Casarella [7], Camussi et al. [12] and Leclerq et al. [13]. Lower Reynolds numbers in other studies cause the reattachment lengths to be lower than those reported in this study and by other researchers at similar δ/h ratios. The current study investigates a broad range of δ/h ratios and the reattachment lengths generally increase as δ/h values decrease. This is consistent with the theory that at low δ/h values, the highest velocity flow interacts with the crest of the FFS, inducing a momentum increase, forcing the separation region farther downstream, resulting in a larger separation region.

The example shown in Figure 6 also illustrates the three-dimensional, cellular nature of the separation region, highlighted by the solid red lines. Castro and Dianat [14] observed similar cellular divisions whilst investigating surface flow topology over rectangular bodies in thick boundary layers at an aspect ratio of 9. They observed a line of symmetry along the model centreline as well as further saddle points relating to the edge effects. Largeau and Moriniere [3] also identified branched structures upstream of their FFS, which provided an inherent three-dimensionality to the flow over the two-dimensional geometry. The branched structures convected downstream over the crest of the FFS as the upstream vortex burst periodically. Largeau and Moriniere [3] observed that these structures occurred symmetrically, and the number of branched structures related to their length, which was a function of the aspect ratio. Other cases in the present study exhibited cell boundaries along the tunnel

centreline and fewer cells. A further distinction between the current study and the work of Castro and Dianat [14] is that the flow tended to funnel towards the centre of the crest (or the centre of the cell, as seen in Figure 6) rather than funneling the flow along the crest, towards the edge of the model. The fixed walls, either of the wind tunnel or of the edge plates, prevented drainage along the edge of the models in the current study.
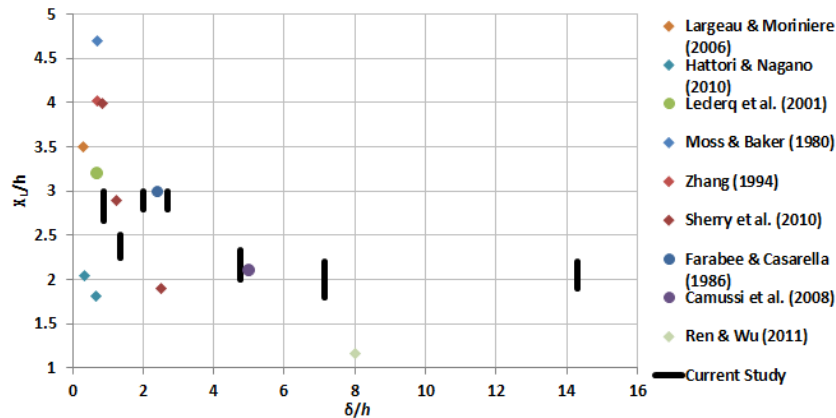

Figure 7. Comparison of mean reattachment lengths with other studies at 0° yaw angle.

4. Effect of yaw angle on the flow over a forward facing step

The effect of yaw angle is broken down into the low TI and the high TI cases. The comparison between the two regimes is presented in Figure 8. The low TI cases are shown in the left pane; the high TI cases are shown in the right pane. For each graph comparisons can be made based on values of δ/h. Comparisons between the two panes, however, need to be considered in terms of a combination of both the TI and δ/h.
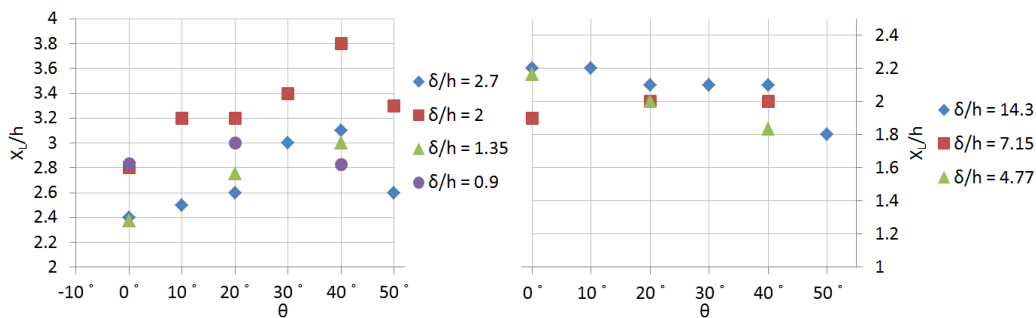

Figure 8. Mean reattachment length as a function of yaw angle for a range of δ/h ratios. Low TI cases shown in the left-hand pane; high TI cases shown in right-hand pane.

Considering first the low TI cases, the $\delta/h = 2$ and $\delta/h = 2.7$ cases were sampled at 10° increments and a consistent trend of increasing X_L with increasing θ is observed. Beyond $\theta = 40°$, a threshold appears to be exceeded, and X_L reduces sharply. The $\delta/h = 1.35$ case exhibits a similar trend in X_L with increasing θ, albeit without an observable threshold, as the highest value of θ was 40° in this case. This trend shows that the lateral flow along the crest increases the stability of the vortex, up to a critical yaw angle.

In addition to X_L, the visualisations give the direction of the surface shear stress lines. The angle these lines make with the stream-wise direction is Ω, which varies linearly as a function of θ, as shown

in Figure 9. The linear relationship is $\Omega = 180 - 2.4\theta$. This relationship was consistent across the low and high TI cases. Note that there is a critical θ where the shear stress lines change from having a counter-stream-wise component (the most extreme case being the recirculation in the $\theta = 0°$ case) to no counter-stream-wise component immediately before $\theta = 40°$. The reduction in Ω with increased θ shows that the crest vortex becomes dominated by the lateral flow, rather than by the low pressure generated by the separation at the crest.

Lateral segmentation was observed in the recirculation region for $\theta = 0°$, as shown in Figure 6. By $\theta = 10°$, this cellular structure in the recirculation region has broken down. However, Figure 10 shows there is a new cellular structure evident in the $\theta = 40°$ and $\theta = 50°$ cases, downstream of the separation region. Streaks indicate distinct regions where the surface shear stress is aligned at an angle of 13° to the direction of the free-stream flow. The orientation of the streaks indicates that a vortex structure of the same sign as the primary vortex structure is being shed from that structure. Because this observation was made in a time-averaged field, it indicates there is a stable spatial periodicity in the shedding from the primary vortex structure.
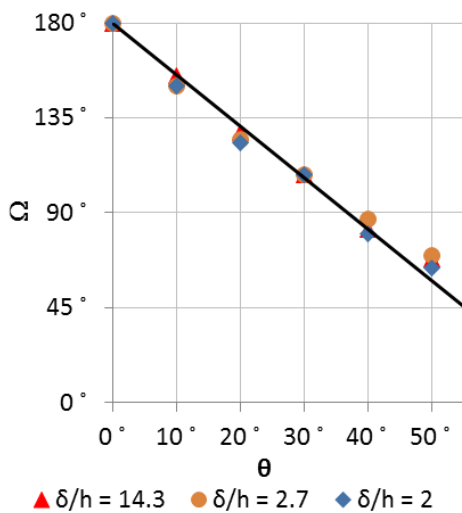

Figure 9. Direction of surface shear stress as a function of yaw. Black line corresponds to linear trend line.
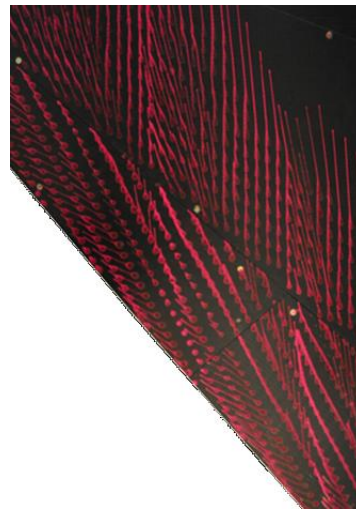

Figure 10. $\theta = 50°$, $\delta/h = 2$ case, showing the segmentation downstream of the separation region. Flow is from bottom of page to top of page.

The high TI cases, whose X_L values are plotted in the right pane of Figure 8, exhibit weaker dependence on θ than the low TI cases. In two of the three δ/h cases, a small reduction in X_L is observed, but the reduction is of a similar order to the magnitude of the uncertainty.

Each of the high TI cases has smaller X_Ls than the low TI cases. The increased TI renders the vortices more unsteady. The reduced momentum and stronger vertical shear associated with the higher values of δ/h compounds the effect.

The downstream shedding that laterally segmented the wake in a spatially periodic manner in the low TI cases was not observed in the high TI cases. The increased turbulence was responsible for breaking down the spatial periodicity.

5. Conclusions
This work describes the effect of yaw angle on flow over an FFS. At a yaw angle of $\theta = 0°$ the results presented here are comparable with similar wind tunnel studies over a range of δ/h.

The mean reattachment length is shown to vary as a function of θ, δ/h and TI. Lateral flow induced by θ is shown to increase the stability of the crest vortex up to a critical value of θ, beyond which the

effect is diminished. When TI was increased and combined with an increase in δ/h, a general decrease in X_L was observed, and further small reductions occurred at higher yaw angles. The increased TI and increase in thickness of the shear layer both promote instability, reducing the ability of the crest vortex to entrain flow.

Vortices generated off the crest of the FFS at different yaw angles are shown to act at an angle relative to the surface, varying linearly with θ, demonstrating a gradual dominance of the lateral flow over the recirculation as θ is increased. This effect was consistent, independent of TI and δ/h.

Distinct segmentation of the flow is observed in the wake of the low TI regimes. At higher TI and δ/h, the segmentation is not obvious, indicating the spatial periodicity is broken down by turbulence.

Acknowledgements

References

[1]   Ren H and Wu Y-T 2011 Turbulent boundary layers over smooth and rough forward-facing steps *Physics of Fluids* **23** 1–17

[2]   Sherry M, Lo Jacono D and Sheridan J 2010 An experimental investigation of the recirculation zone formed downstream of a forward facing step *J. Wind Eng. Ind. Aero.* **98** 888–94

[3]   Largeau J F and Moriniere V 2006 Wall pressure fluctuations and topology in separated flows over a forward-facing step *Experiments in Fluids* **42** 21–40

[4]   Moss W and Baker S 1980 Re-circulating flows associated with two-dimensional steps *Aeronautical Quarterly* **32** 693–704

[5]   Mohsen M 1967 Experimental investigation of the wall pressure fluctuations in subsonic separated flows, (Renton: Boeing Commercial Airline Co.)

[6]   Tashie M F, Balachandar R and Bergstrom D J 2001 Open channel boundary layer relaxation behind a forward facing step at low Reynolds numbers *J. of Fluid Eng.* **123**: 539-544

[7]   Farabee T M and Casarella M J 1991 Spectral features of wall pressure beneath turbulent boundary layers *Phys Fluids* **3** 2410–20

[8]   Baker C J 1985 The determination of topographical exposure factors for railway embankments *J. Wind Eng. Ind. Aero.* **21**: 89-99

[9]   Kiya M and K Sasaki 1983 Structure of a turbulent separation bubble *J. of Fluid Mechanics* **137** 83-113

[10]   de Brederode V and Bradshaw P 1972 Three-dimensional flow in nominally two-dimensional separation bubbles: Flow behind a rearward-facing step. *I.C. Aero Report.* (London: Imperial College of Science and Technology) **72** 100

[11]   AS/NZS (2011). Structural design actions. Part 2: Wind actions. Sydney, Wellington, *Standards Australia/Standards New Zealand.* AS/NZS 1170.2:2011: 99.

[12]   Camussi R, Felli M, Pereira F, Aloisio G and Di Marco A 2008 Statistical properties of wall pressure fluctuations over a forward facing step *Physics of Fluids* **20** 075113-1-13

[13]   Leclercq D, Jacob M, Louisot A and Talotte C 2001 Forward-backward facing step pair: Aerodynamic flow, wall pressure and acoustic characterisation *7th AIAA/CEAS Aeroacoustics Conference and Exhibit paper n° 2001-2249* (Maastricht: AIAA)

[14]   Castro I P and Dianat M 1983 Surface flow patterns on rectangular bodies in thick boundary layers *J. Wind Eng. Ind. Aero.* **11** 107-119